LA-UR--85-2991

DE85 017540

SEP 1 0 1985

CONF-8509202--1

TITLE: STUDIES OF NUCLEAR STRUCTURE VIA POLARIZATION TRANSFER EXPERIMENTS

AUTHOR(S): J. M. Moss

SUBMITTED TO: Proceedings of 1985 RCNP-KIKUCHI Summer School, Osaka, Japan, September 1985

DISCLAIMER

Los Alamos Los Alamos National Laboratory
Los Alamos, New Mexico 87545

STUDIES OF NUCLEAR STRUCTURE VIA POLARIZATION TRANSFER EXPERIMENTS

J. M. Moss

Los Alamos National Laboratory
Los Alamos, New Mexico

1. INTRODUCTION

The most important development in nucleon-nucleus physics in recent years is the advent of polarization transfer experiments. By measuring much more than the standard cross section and analyzing power in (p,p′) and (p,n) reactions, one is finally able to exploit the spin complexity of the NN interaction to investigate a wide range of physics problems.

The impact of polarization transfer has been most dramatic in the medium-energy range (E_p > 100 MeV) where the longer range of protons make feasible the construction of very efficient polarimeters. Focal plane polarimeters have been in common use for (p,p′) studies for several years at LAMPF[1] and IUCF.[2] At IUCF recently developed neutron polarimeters have made notable contributions to the study of (p,n) reactions.[3,4]

In this talk I will concentrate on inelastic scattering and charge exchange reactions at medium energies. Section 2 discusses experiments dealing with discreet nuclear states. As background I will briefly introduce relevant theoretical considerations. In this section I will also give some personal views on where such studies seem to be headed, with particular emphasis on future tests of model's based on the Dirac equation. The origin of spin-current couplings "appears" very different in present Dirac versus Schroedinger based models and is thus a prime target for spin-observable experiments. Further, only in inelastic experiments is one able to examine the complete range of couplings* present in the Dirac representation of the NN amplitude.

In Sec. 3 I will discuss in detail a recent LAMPF experiment in which polarization observables were employed to make a very precise search for collective effects in the nuclear pion field. This experiment has an interesting connection to the famous EMC (European Muon Collaboration) effect since pionic collectivity has been proposed as an explanation of this ultra high-energy scattering experiment.

---

*These are scalar, vector, tensor, pseudoscalar, and axial vector.

2. POLARIZATION TRANSFER TO DISCREET STATES

Theoretical Background

In the most general distorted-waves formulation the expressions for the various polarization transfer observables are very complex. Fortunately in recent years a great deal of attention has been focused on deriving approximate expressions where the physics content of the spin observables is much more transparent.[5-8] This has been done in the context of both the Schroedinger and Dirac equations. A notable by-product of these analyses has been a much more obvious connection between the effective one-body operators of nucleon scattering and those appearing in electromagnetic and semi-leptonic weak interaction transitions.

In this talk I will use the simplest of the approximate forms. In this model the transition amplitude for N-nucleus scattering is

$$\bar{M}_{J\mu} = \langle J\mu | M(q) e^{-i\hat{q}\cdot\hat{r}} | 0 \rangle \qquad (1)$$

where M(q) is the NN acattering amplitude, and μ is the projection of the total angular momentum transfer J along the q axis. Specifically

$$M(q) = A + B\sigma_{1n}\sigma_{2n} + C(\sigma_{1n} + \sigma_{2n}) + E\sigma_{1q}\sigma_{2q} + F\sigma_{1p}\sigma_{2p}$$

with $\hat{n} = \hat{k} \times \hat{k}'$, $\hat{q} = \hat{k}' - \hat{k}$, and $\hat{p} = \hat{q} \times \hat{n}$; $\hat{k}$ ($\hat{k}'$) is the incident (outgoing) nucleon momentum. Equation 1 is the plane-wave Born approximation if one calculates cross sections. For spin observables, however, it implies only local plane waves since an assumed nuclear attenuation factor (spin-independent) would factor out; thus Eq. 1 is more accurately described as the eikonal form. Using standard methods to evaluate the spin observables one finds for the cross section and the diagonal spin observables for

(a) unnatural parity states

$$\sigma_o D_{nn} = \Sigma_J^2(C^2 + B^2 + F^2) - \Sigma_L^2 E^2 \quad . \qquad (2a)$$

$$\sigma_o D_{qq} = \Sigma_J^2(C^2 - B^2 - F^2) + \Sigma_L^2 E^2 \quad , \qquad (2b)$$

$$\sigma_o D_{pp} = \Sigma_J^2(C^2 - B^2 + F^2) - \Sigma_L^2 E^2 \quad , \qquad (2c)$$

$$\sigma_o \quad = \Sigma_J^2(C^2 + B^2 + F^2) + \Sigma_L^2 E^2 \quad , \qquad (2d)$$

and for

(b) natural parity states

$$\sigma_o D_{nn} = \tfrac{1}{2}\Sigma_J^2(C^2 + B^2 - F^2) + \rho^2(A^2 + C^2) \quad , \qquad (3a)$$

$$\sigma_o D_{qq} = \tfrac{1}{2}\Sigma_T^2(C^2 - B^2 - F^2) + \rho^2(A^2 - C^2) \quad , \tag{3b}$$

$$\sigma_o D_{pp} = \tfrac{1}{2}\Sigma_T^2(C^2 - B^2 + F^2) + \rho^2(A^2 - C^2) \quad , \tag{3c}$$

$$\sigma_o = \tfrac{1}{2}\Sigma_T^2(C^2 + B^2 + F^2) + \rho^2(A^2 + C^2) \quad . \tag{3d}$$

In the approximations we have used there are no spin-current couplings of the two nucleons, with the result that there are only three nuclear matrix elements. They are

$$\text{spin transverse, } \Sigma_T = \langle \mu | \hat{\sigma} \times \hat{q} e^{-i\vec{q}\cdot\vec{r}} | 0 \rangle \quad , \tag{4a}$$

$$\text{spin longitudinal, } \Sigma_L = \langle \mu | \hat{\sigma} \cdot \hat{q} e^{-i\vec{q}\cdot\vec{r}} | 0 \rangle \quad , \tag{4b}$$

$$\text{and scalar, } \rho = \langle \mu | e^{-i\vec{q}\cdot\vec{r}} | 0 \rangle \quad . \tag{4c}$$

In spite of the simple assumptions made these equations provide a reasonably quantitative view of much of the existing polarization transfer data; they also reproduce many of the major features of much more complex DWBA calculations. We give two examples as illustrations.

Applications of the Simple Model

First it is clear from Eqs. 2 and 3 that the transverse spin-flip probability, $S_{nn} = (1 - D_{nn})/2$, isolates spin-dependent matrix elements uniquely. This is made clearer by rewriting Eq. 3a as

$$S_{nn} = \Sigma_T^2 F^2 / 2\sigma_o \quad .$$

Thus a "spin-flip" spectrum $S_{nn}\sigma_o$ suppresses collective spin-independent transitions. This is very clearly observed in the spectrum of Fig. 1. The use of S_{nn} as a spin-flip filter has been employed in studies of the continuum surrounding the M1 resonance region excited in (p,p′) reactions[10] and in (p,n) studies of the giant Gamow-Teller resonance.[3]

As a second example of the utility of Eqs. 2 and 3 we examine the excitation of the $1^+T=1$ state in ^{12}C by 500 MeV protons. At the small momentum transfer shown in Fig. 2 the spin transverse and spin longitudinal form factors are proportional since $\ell = 0$ is dominant. In this case one then has

$$D_{nn} = \frac{C^2 + B^2 + F^2 - E^2}{C^2 + B^2 + F^2 + E^2} \quad .$$

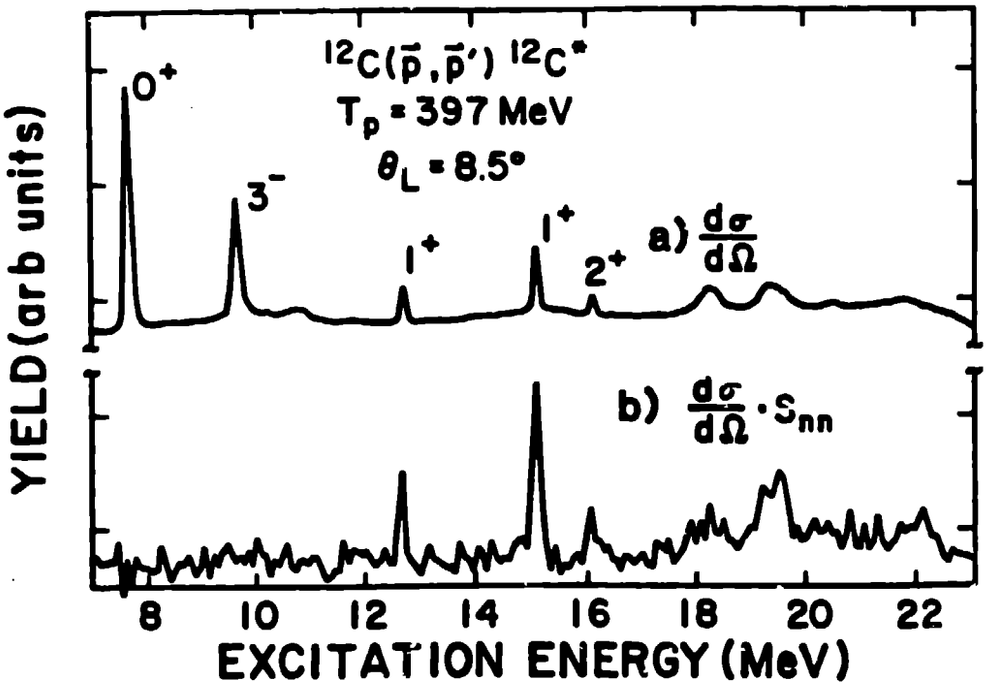

Fig. 1. Cross section and spin-flip cross section spectrum from Ref. 9.

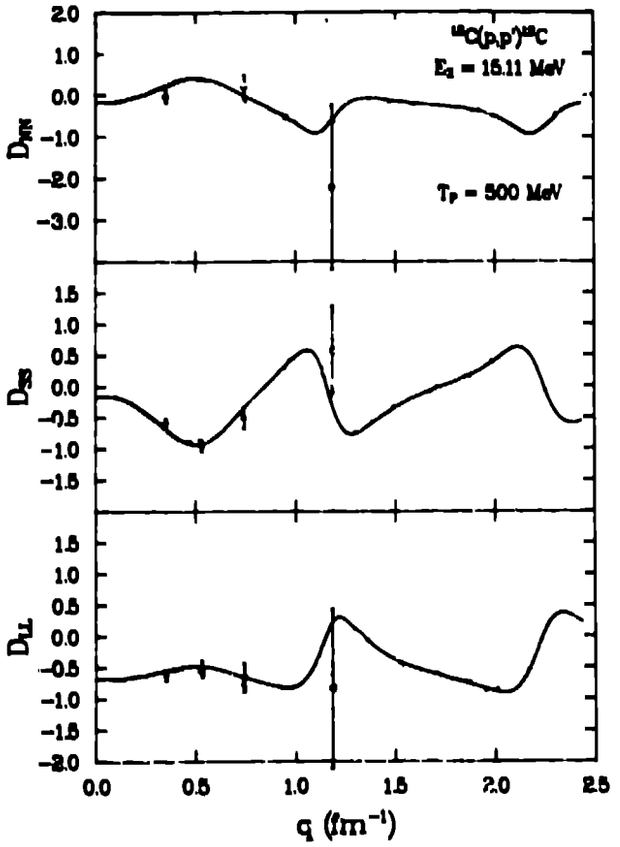

Fig. 2. Polarization transfer observables for $^{12}C(p,p')^{12}C(1^+,T=1)$ (from Ref. 1). The curves is a calculation using the model described in the text.

Similar expressions hold for the other observables but are more complex due to the center-of-mass to laboratory transformation.[5] It is clear that the nuclear structure divides out and one is left with an expression which can be used to test the impulse approximation interaction. The simplest form of this interaction is obviously adequate to describe these data. Further examples of polarization transfer calculations applied to experiment are given in recent review talks by Carey[11] and Taddeucci[12] at the Osaka Polarization Conference.

Future Directions

One of the most important developments in Nuclear Physics in recent years is the successful application of models based on the Dirac equation to a variety of N-nucleus problems.[13] As you are undoubtedly aware much of the impetus for the Dirac approach arose from the spectacular failure of standard Schroedinger-based theory to account for polarization transfer data in elastic scattering. It has been often pointed out that the feature which makes the Dirac approach so different in its description of N-nucleus processes is the presence of a strong attractive scalar (S) and a strong repulsive vector (V) potential. The quantity S - V which "makes relativity important" is thus large.

Tests of Dirac Equation Models

Elastic polarization experiments, which gave rise to the current interest in the use of the Dirac equation, have a limited potential for future tests of theory. Of the five terms which appear in the NN scattering amplitude for NN scattering, only S and V significantly affect the elastic channel (there is also a small tensor term which is often ignored). If one wants to look at the axial vector (A), pseudoscalar (P), and sensitivity at the tensor (T) terms, inelastic or charge-exchange experiments are required -- not just any inelastic experiments, of course, but those which involve spin excitations. These are often states with small cross sections. Further to be a real test of any theory, as we have learned from the case of elastic scattering, precise data are necessary. Qualitative improvements in polarized-ion source intensity and polarimeter efficiencies are probably necessary to accomplish this.

Spin Current Coupling: An Example

Much attention has been devoted recently to the effective one-body operators which enter the description of N-nucleus scattering from both the Dirac and Schroedinger equation approaches.[7,8,14,15] Terms beyond those of Eqs. 4 which involve current and spin-current coupling are clearly allowed in both approaches. The origins of such terms, however, may be quite different in the two types of models. The "may be" qualifier is appropriate here because progress is still being made in understanding the differences and similarities of the two approaches. With the assumption that real differences will remain when all is understood, I will speculate that experiments such as P-A may provide the critical evidence necessary to choose the "right" model.

The polarization and analyzing power are identical for inelastic transitions in the model outlined earlier where only static NN interactions are considered (distortion effects coupled with non-zero Q values give rise to small differences between P and A). Spin current couplings, however, provide driving terms which lead directly to inequalities between P and A. The action of operators of the type $\hat{\sigma}\cdot\hat{j}e^{-iq\cdot r}$ and $\hat{\sigma}\times\hat{j}e^{-iq\cdot r}$ are seen in such measurements. Figure 3 shows P-A data at 150 MeV for the $1^+T=0$ state of ^{12}C compared with several calculations described in detail in Ref. 15.

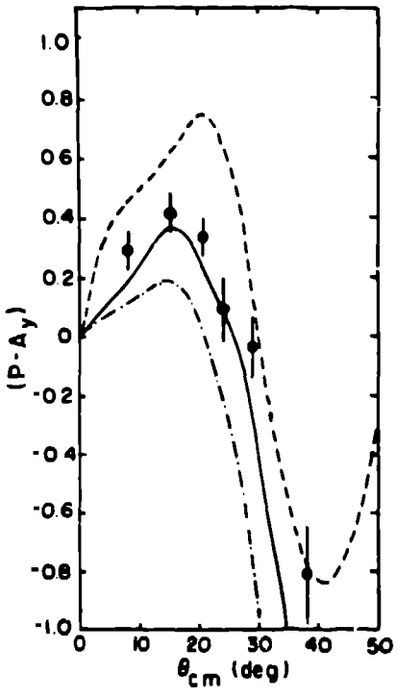

Fig. 3. Polarization minus analyzing power data. The solid and dot-dashed curves are Dirac model calculations. The dashed curve uses a Schroedinger equation-based model. The curves are described in detail in Ref. 15.

It is much too early to say which (if any) calculation is favored by the data. It does seem clear, however, that more and much better data are required for observables which are particularly sensitive to spin-current couplings. In the confrontation of such hypothetical data with calculation it is unlikely that both the Dirac- and Schroedinger-based approaches will survive.

3. THE EMC EFFECT AND POLARIZATION TRANSFER

In this section I will give a brief introduction to the EMC effect[16] and its interpretation in terms of excess nuclear pions.[17-20] This model establishes a connection between the vastly different scales of the EMC experiment (~200 GeV deep-inelastic muon scattering) and the Los Alamos experiment (500 MeV polarized-proton quasifree scattering). Following this I will describe the Los Alamos experiment and its interpretation in terms of excess nuclear pions. Finally I will indulge in some speculation about quark effects in nuclei based on the EMC and Los Alamos experimental results.

Figure 4 shows the EMC results in terms of the ratio of the F_2 structure functions of iron and deuterium (assumed to represent a free neutron and proton target) as a function of the scaling variable, x.[21] If nucleons in a nuclear target behaved as an assembly of A free nucleons, this ratio would be unity over the entire range of x (neglecting small Fermi motion effects). It is obviously not; thus the EMC result is telling us, viewed even at these ultra high energies, that nuclei have some very interesting structure. Attempts to understand this structure have inspired more than 20 theoretical papers in the past two years. These theoretical efforts may be classified roughly in two different categories: those which invoke some <u>new quark-level</u> physics in nuclei, and those which attribute the EMC effect to excess nuclear pions--a "conventional" many-body enhancement employing meson, nucleon, and isobar degrees-of-freedom, and hence <u>not requiring</u> new quark effects in

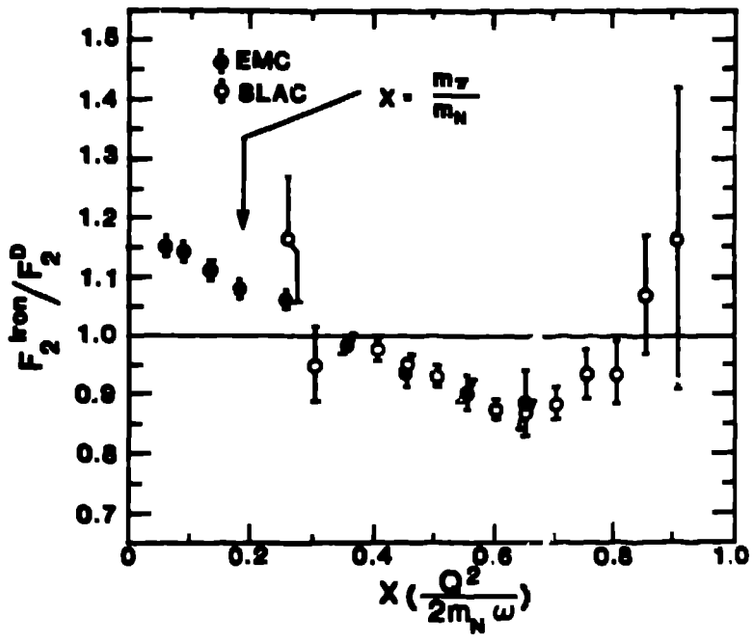

Fig. 4. Deep-inelastic lepton scattering from the EMC group and older SLAC data.

nuclei. Models of the first type typically contain parameters which allow one to obtain the EMC effect through quark-level mechanisms--the magnitude of this mechanism usually remains to be explained. The enhanced pion field calculation, on the other hand, can be done with no free parameters.

Figure 5 summarizes the ideas underlying the pionic enhancement model. Briefly, deep-inelastic lepton scattering (DILS) at very high energies is described in terms of the electromagnetic interaction between leptons and quarks.[22] These may be valence quarks, those determining the charge, baryon number, etc., of the nucleon, or sea quarks, arising from symmetric $q\bar{q}$ excitations. As an example of sea-quark scattering (Fig. 5b), a photon can interact with the q or $\bar{q}$ of a virtual pion. This can happen in free-nucleon DILS since the experiment is inclusive with no observation of the final nuclear state. In nuclear matter, the πNN vertex has the possibility of being enhanced by the process shown in Fig. 5c. Such an enhancement, resulting from an attractive NN interaction in the pionic or isovector spin-longitudinal channel, would yield excess pions from which high-energy leptons could scatter. Viewing the nucleus as an assembly of nucleons and pions, a pion excess leads naturally to enhanced scattering in the region $x = m_\pi/m_N$ (the kinematic point where elastic muon-pion scattering would take place). In the original pion-excess model of Llewellyn-Smith[17] it is shown that the EMC effect extrapolated to x = 0 is roughly the fractional pion excess in iron

$$f^{iron} = \frac{F_2^{iron}(x=0)}{F_2^D(x=0)} - 1 \quad .$$

Thus the original EMC data imply $f^{iron} = 0.15$.

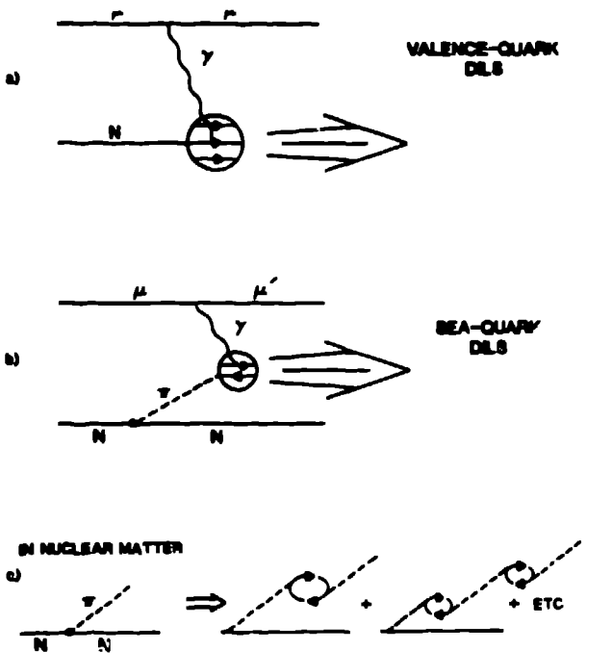

Fig. 5. Diagrams for deep-inelastic lepton scattering (a and b). Possible enhancement of the πNN vertex is shown in c.

The Pion Excess Model and 500 MeV Proton Scattering

The relation between the EMC experiment and the Los Alamos experiment is shown schematically in Fig. 6. In both reactions one seeks evidence of a many-body enhancement at πNN vertex. The experiments are obviously unrelated except through a common interpretation in terms of the enhanced pion field model. In the former case the model provides excess $q\bar{q}$ pairs from which high-energy lepton can scatter; in the latter, it provides pions which can be more readily exchanged between an incoming nucleon and the nucleons of the nucleus. To make clear the role of the isovector spin-longitudinal response function in the description of both experiments we summarize the appropriate equations below (as given by Ericson and Thomas, Ref. 18, for the EMC effect). For DILS one calculates the pionic contribution to the F_2 structure function of iron by folding the pion intensity function h(y) with the pion structure function, F_2^{π}, viz.,

$$\delta F_2(x) = \int_x^1 h(y)\, F_2^{\pi}\left(\frac{x}{y}\right) dy \qquad (5)$$

with

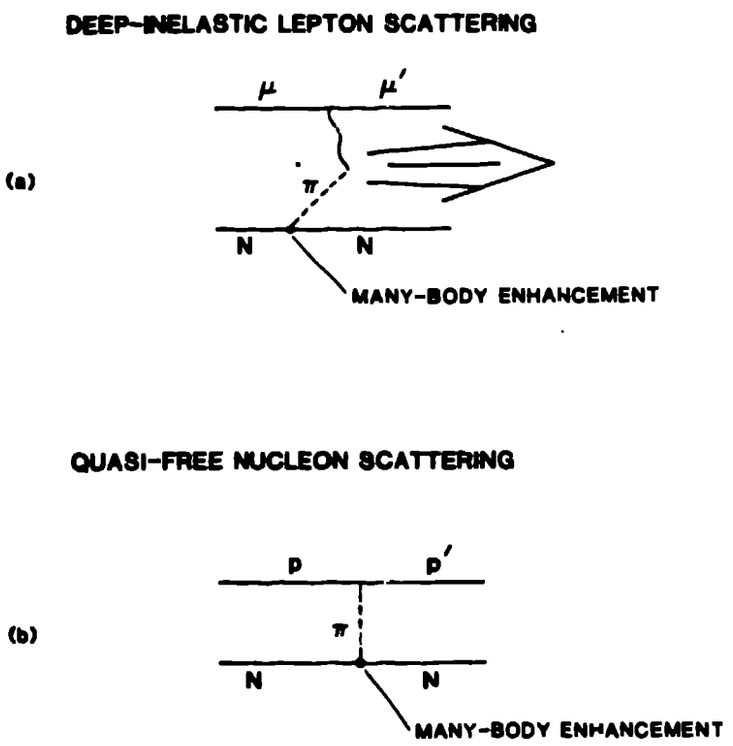

Fig. 6. Schematic relation between lepton and nucleon scattering in the pion excess model.

$$h(y) = \frac{3g^2}{16\pi^2} \int_{m_N^2}^{\infty} \frac{y^2}{1-y} \int_0^{q-m_N y} dq^2 d\omega \, \frac{q^2 |F(q^2)|^2 R_L(q,\omega)}{(q^2 - \omega^2 + m_\pi^2)^2} \tag{6}$$

where g is the coupling constant and $F(q^2)$ the form factor at the πNN vertex.

In the description of the isovector spin-longitudinal (pion-exchange) scattering of nucleons by nuclei one has

$$\sigma_L^{NA} = \sigma_L^{NN} N_e R_L(q,\omega) \tag{7}$$

where σ_L^{NA} and σ_L^{NN} are respectively the spin-longitudinal cross sections for NA and NN scattering, N_e is an effective number of nucleons, and $R_L(q,\omega)$, the isovector spin-longitudinal response function which also appears in Eq. 6. More detail about Eq. 7 and the experimental determination of σ_L is given below.

Inclusive Quasifree Scattering and $R_L(q,\omega)$

There are two features which set our experiment apart from others which have used the nucleon as a probe of pionic effects.

First, as in the EMC experiment, our point of reference is deuterium. We compare the spin-dependent response functions for a heavy target (Pb in our case) and ^2H using identical experimental techniques. If the predicted many-body effects are present in Pb even at a very small level, they should be detectable in a precise ratio experiment.

Second, we use the technique of complete polarization transfer[23] to separate the spin-longitudinal ($\vec{\sigma}\cdot\vec{q}$) and spin-transverse ($\vec{\sigma}\times\vec{q}$) response in the continuum as a function of ω (across the entire quasielastic peak, ω = 20 to 100 MeV). The responses are measured at a momentum transfer $q = 1.75$ fm^{-1} which corresponds to the maximum predicted enhancement of $R_L(q,\omega)$ in most models.

The experiment consists of precise determinations of the polarization transfer coefficients D_{LL}, D_{SS}, and D_{NN} for 500 MeV protons inelastically scattered from Pb and ^2H at $q = 1.75$ fm^{-1}. The experiment utilized longitudinal (L), sideways (S), and normal (N) polarized beams from LAMPF in conjunction with final polarization analysis from the focal-plane polarimeter of the high-resolution spectrometer. The quantities constructed from the above data are the longitudinal and transverse spin-flip probabilities defined by

$$S_L = \frac{1}{4}\left(1 - D_{NN} + (D_{SS} - D_{LL})\sec\theta_{lab}\right) ,$$

$$S_T = \frac{1}{4}\left(1 - D_{NN} - (D_{SS} - D_{LL})\sec\theta_{lab}\right) .$$

The free NN scattering amplitude is written as in Sec. 1 as

$$M(q) = A + B\sigma_{1n}\sigma_{2n} + C(\sigma_{1n} + \sigma_{2n}) + E\sigma_{1q}\sigma_{2q} + F\sigma_{1p}\sigma_{2p} ,$$

where the σ's are projections of the Pauli spinors along $\hat{n} = \hat{k} \times \hat{k}'$, $\hat{q} = \hat{k}' - \hat{k}$, and $\hat{p} = \hat{q} \times \hat{n}$; $\hat{k}(\hat{k}')$ is the incident (outgoing) nucleon momentum direction. The spin-longitudinal and transverse cross sections can be formed by

$$\sigma_L^{NN} \equiv I^{NN}S_L^{NN} = E^2 ,$$

$$\sigma_T^{NN} \equiv I^{NN}S_L^{NN} = F^2 , \qquad (8)$$

with

$$I^{NN} = A^2 + B^2 + 2C^2 + E^2 + F^2 .$$

Here I^{NN} is the differential cross section. Obviously for NN scattering the

combinations for σ_L and σ_T isolate pure spin-longitudinal and spin-transverse couplings of the two-nucleon interaction.

For medium-energy nucleon-nucleus interactions we take the following ansatz

$$IS_L = I^{NN}S_L^{NN}R_L(q,\omega)N_e$$

$$IS_T = I^{NN}S_T^{NN}R_T(q,\omega)N_e \qquad (9)$$

$$I = I^{NN}R(q,\omega)N_e$$

with the spin-longitudinal, transverse, and total response functions defined as

$$R_L(q,\omega) = |\langle q,\omega|\vec{\sigma}\cdot\hat{q}\ e^{-i\vec{q}\cdot\vec{r}}|0\rangle|^2 \quad ,$$

$$R_T(q,\omega) = |\langle q,\omega|\vec{\sigma}\times\hat{q}\ e^{-i\vec{q}\cdot\vec{r}}|0\rangle|^2 \quad ,$$

$$R(q,\omega) = \frac{C^2 + B^2 + F^2}{I^{NN}} R_T + \frac{E^2}{I^{NN}} R_L + \frac{A^2 + C^2}{I^{NN}} R_0 \quad ,$$

where

$$R_0 = |\langle q,\omega|\ e^{-i\vec{q}\cdot\vec{r}}|0\rangle|^2 \quad .$$

N_e is the effective number of participating nucleons as defined by Bertsch and Scholten.[24] The approximations implied in Eqs. 8 and 9 are well satisfied for forward-angle scattering of 500 MeV protons.[24-26]

With the assumption that scattering from deuterium represents free pp plus pn scattering, we have $S^D = S^{NN}$, and from Eqs. 8 and 9 one finds

$$S_L^{Pb}/S_L^D = R_L(q,\omega)/R(q,\omega) \quad , \qquad (10)$$

$$S_T^{Pb}/S_T^D = R_T(q,\omega)/R(q,\omega) \quad , \qquad (11)$$

and

$$\frac{S_L^{Pb}/S_L^D}{S_T^{Pb}/S_T^D} = R_L(q,\omega)/R_T(q,\omega) \quad . \tag{12}$$

Thus the simple ratios (Eqs. 10 and 11) depend only on ratios of response functions for Pb. The super ratio of Eq. 12 can be used to contrast the two spindependent response functions of Pb.

The experimental spin-flip probabilities for Pb and ^{2}H are shown in Fig. 7. It is clear that there is no evidence of many-body enhancement in the spin-longitudinal channel (Fig. 7a) since there is no significant difference between Pb and ^{2}H. Likewise in the transverse channel we see no evidence of collective behavior. This is consistent with what is known of the transverse response function in this range of momentum transfer as derived from inclusive (e,e′) experiments.[27]

The question that remains to be settled is, what is the sensitivity of the present experiment to excess pions or equivalently to collectivity in the isovector spin-longitudinal response.

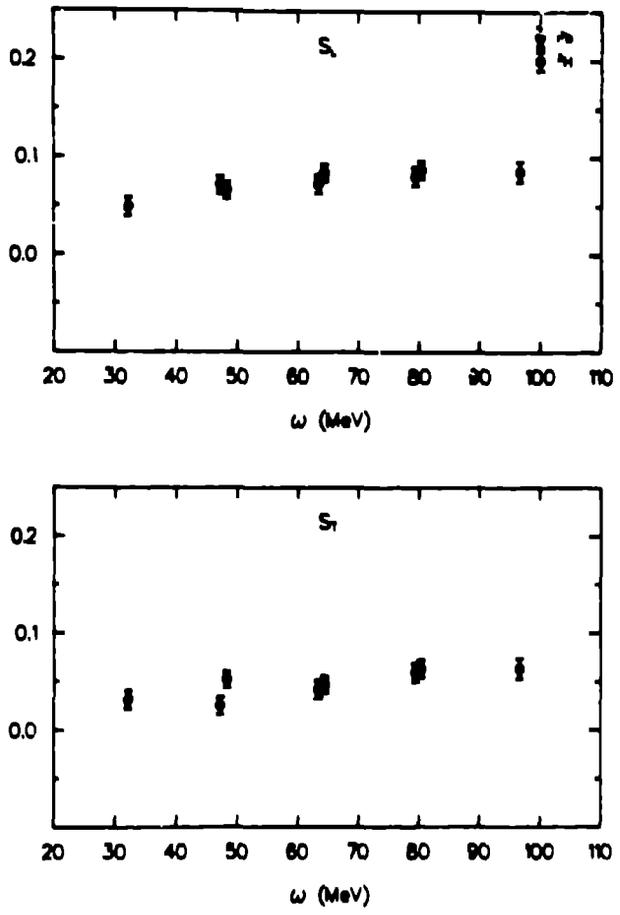

Fig. 7. Longitudinal and transverse spin-flip probabilities for Pb and ^{2}H at q = 1.75 fm^{-1}.

Spin-Isospin Response Functions

Calculation of the spin-isospin responses in this work follows the methods used by Alberico, Ericson, and Molinari (AEM).[28,29] Even though our primary interest is in the spin-longitudinal response we consider the transverse as well since, as suggested by AEM, much of the theoretical uncertainty associated with the use of infinite nuclear matter should disappear if one analyzes the ratio R_L/R_T. The response functions are calculated in infinite nuclear matter using the random-phase approximation (RPA). The NN interaction in the longitudinal channel is taken to be a mixture of one-pion-exchange plus a repulsive short-range repulsion represented by the usual Fermi liquid parameter g_0'. The transverse force is a combination of rho-meson exchange and g_0'. With a "reasonable" value of $g_0' = 0.7$, the behavior of the NN interactions and the associated response functions in the range $q = 1.78$ fm^{-1} are shown in Fig. 8. The (proposed) attractive behavior of V_L^{ph} at $q \sim 2$ fm^{-1} results in an enhancement and a softening (shift to lower energies) of R_L. In contrast the repulsive behavior of V_T^{ph} leads to a quenching and hardening of R_T with respect to the free Fermi-Gas response. An alternative interaction favored by the Jülich/Stony Brook/Saclay school[30] would not produce an enhancement in R_L and consequently no excess pions for the EMC effect.

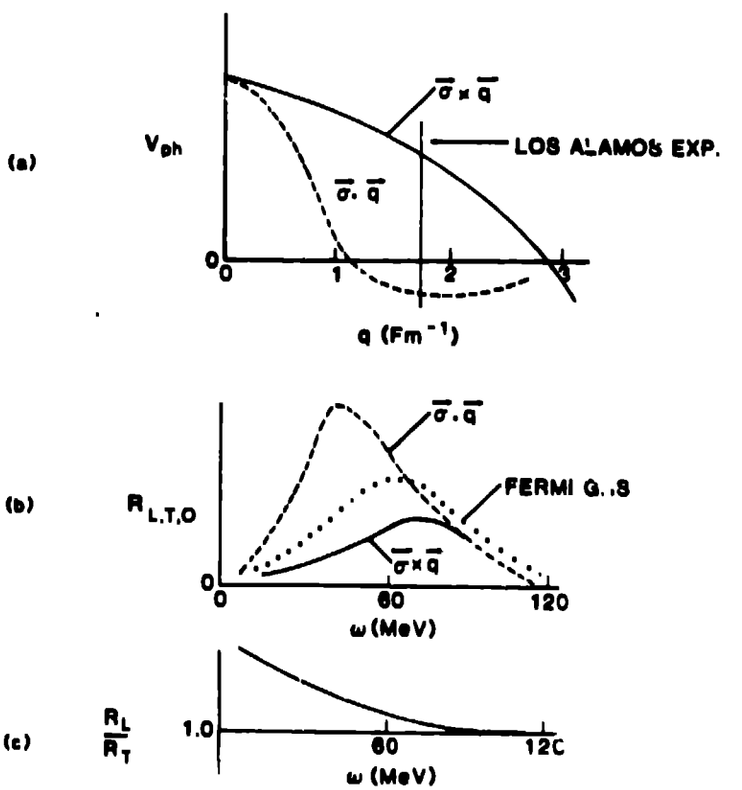

Fig. 8. (a) Longitudinal and transverse particle-hole interactions in the model described in the text. (b) Response functions at $q = 1.75$ fm^{-1} from the interactions shown above. (c) Ratio of longitudinal to transverse response functions.

Calculation of R_L, R_T for 500 MeV Protons

To compare the results of the infinite nuclear matter calculations of the response functions to experiment one uses the local-density approximation.[24,28] This is accomplished in a somewhat different fashion for protons than for weakly interacting leptons which see the entire nuclear volume. The method we employ is to generate a sensitivity profile--an interaction probability versus radius for 500-MeV protons interacting with Pb and producing outgoing protons at the appropriate scattering angle. This is accomplished via an intranuclear cascade calculation[31] the results of which are shown in Fig. 9. For comparison we also show the sensitivity profile, $r^2\rho(r)$, for a weakly interacting probe. The profile for protons is then folded together with RPA calculations performed at the appropriate nuclear density. The resulting response functions are similar to those obtained by a proton sampling the nucleus at an average density $\rho = 0.45\rho_0$. Further details of the averaging procedure, including the method of handling the neutron excess for Pb, will be described in a forthcoming publication.[32]

The mixed isospin nature of the (p,p′) reaction must also be accounted for in comparing to theoretical models of the pure spin-isospin responses.[29] This is accomplished by analyzing the 500-MeV NN phase-shift solutions[33] in terms of isospin components. The results at $q = 1.75$ fm^{-1} are

$$\sigma^{NN}_{T=1}/\sigma^{NN}_{T=0} = 3.62 \text{ for longitudinal}$$

$$\sigma^{NN}_{T=1}/\sigma^{NN}_{T=0} = 1.15 \text{ for transverse}$$

Calculation of the isoscalar responses rely on the reasonably well-established observation that the residual spin-dependent force in the nucleus in this channel is very weak.[34] The corresponding response functions, $R_L^{T=0}$, $R_T^{T=0}$,

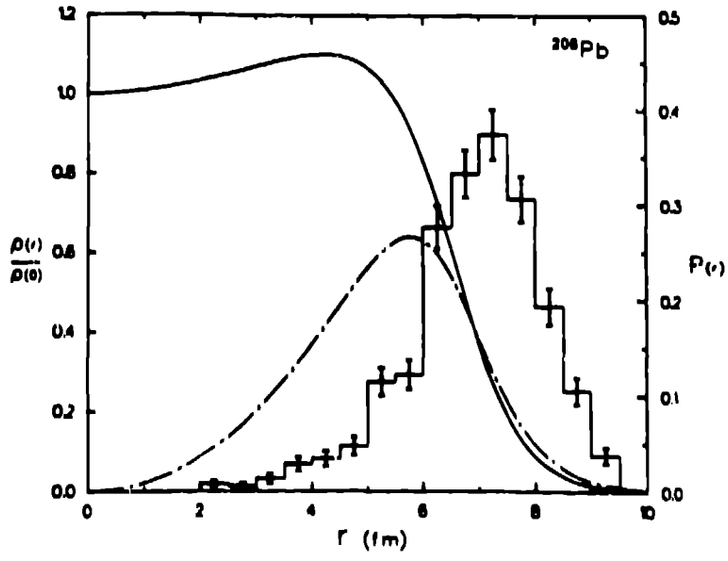

Fig. 9. Sensitivity profile of 500 MeV protons interacting with ^{208}Pb and producing protons at 18.5° in the lab system (histogram with associated points). Also shown are $r^2\rho(r)$ and $\rho(r)$ for ^{208}Pb.

are hence taken to be those of a free Fermi Gas. The quantities compared with experiment are then:

$$\tilde{R}_L = \frac{1}{4.62}\,(3.62\ R_L^{T=1} + R_L^{T=0})$$

$$\tilde{R}_T = \frac{1}{2.15}\,(1.15\ R_T^{T=1} + R_T^{T=0})$$

The results of these calculations with the values of Fermi parameter $g_0' = 0.10$ and 0.9 are shown in Fig. 10 (dashed and dot-dashed curves). Included in the data set are the five points published previously[23] and a new point at $\omega = 19$ MeV (this is not included in Fig. 10a where the data are averaged over ω). Although the predicted enhancement in $\tilde{R}_L/\tilde{R}_T$ is only modest with the original parameters ($g_0' = 0.7$) used by Ericson and Thomas,[18] one still sees no evidence for it in our data. When g_0' is raised to 0.9 virtually all collectivity in R_L disappears resulting in better agreement with our data but virtually no excess pions for this model of the EMC effect.

Objections have been raised[35] about the validity of the infinite nuclear matter--local Fermi-Gas calculations in the range $\omega < 40$ MeV, precisely where the deviation of theory from experiment is greatest. We believe these objec-

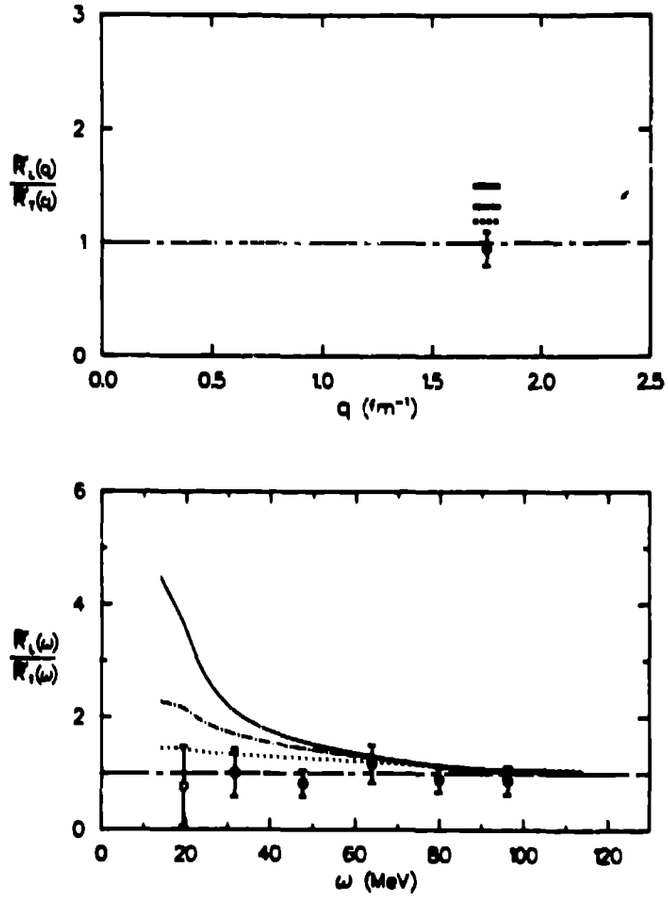

Fig. 10. Comparison of theory and experiment for the ratio R_L/R_T (integrated over ω in (a)). The calculations are for values of $g_0' = 0.55$ (solid), $g_0' = 0.7$ (dashed), and $g_0' = 0.9$ (dotted).

tions are unfounded for the following reasons. First, there is convincing experimental evidence that even the simplest Fermi-Gas calculation[24,26] accounts reasonably well for continuum (p,p′) cross sections (roughly the spin independent response, R_0) down to the region of strong giant resonances ($\omega < 20$ MeV). A more sophisticated version of the model,[24,26] the semi-infinite slab approximation, quantitatively reproduces the shape and cross section of the continuum in this region. Second, because we analyze only ratios of response functions, even the remaining shortcomings of the Fermi-Gas model are unimportant. Esbensen and Bertsch[34] have shown that the local Fermi-Gas treatment of R_L/R_T accurately follows a more sophisticated calculation where binding energy effects are included--even in the range $\omega \sim 20$ MeV.

Further evidence against pions as the dominant source of the low-x EMC effect comes from more recent calculations by Berger et al.,[20] Stump et al.,[19] and by Ericson and Thomas.[35] These calculations take more careful account of the momentum balance in the pion excess model of deep-inelastic lepton scattering. The result is that even the modest value of $g_0' = 0.7$ gives insufficient enhancement at small x ($x < 0.3$) to reproduce the EMC effect. Stump et al. favor a value in the range $g_0' = 0.55$ in order to obtain the magnitude of the low-x EMC effect. As is obvious from Fig. 10 (solid curve) such an enhancement in R_L is completely inconsistent with our data.

Summary and Conclusions

We find no evidence for collectivity in the isovector spin-longitudinal response function from a comparison of 500-MeV proton scattering from Pb and ^{2}H (Fig. 7). On the basis of our best analysis of the 500-MeV proton scattering data, excess nuclear pions are unlikely to be the dominant source of the low-x EMC effect. To be semi-quantitative, our experiment is consistent with no more than 0.05 excess pions as the source of the EMC effect in iron. Recalling that the intercept $(1 - F_2^{iron}/F_2^D)_{x=0}$ is roughly this fraction, one must look elsewhere to understand the low-x EMC enhancement. This, of course, leaves a variety of quark-level nuclear structure explanations of the EMC experiment[33]--a more exciting prospect if one is after real evidence of quark physics in nuclear structure.

To close, allow me to use a rather simple-minded figure (Fig. 11) to illustrate the complementarity of our experiment and that of the EMC. It is a complementarity that may need to be brought to bear for future experimental searches for quark effects in nuclear structure. High-energy experiments certainly probe quarks (and gluons) in nuclei. But the traditional degrees of freedom of nuclei, nucleons and mesons, may also be relevant to the description of even these very high-energy processes. Only by combining the views of nuclei provided by very short and relatively longer wavelength will we be able to choose the most appropriate degrees of freedom for describing nuclear structure.

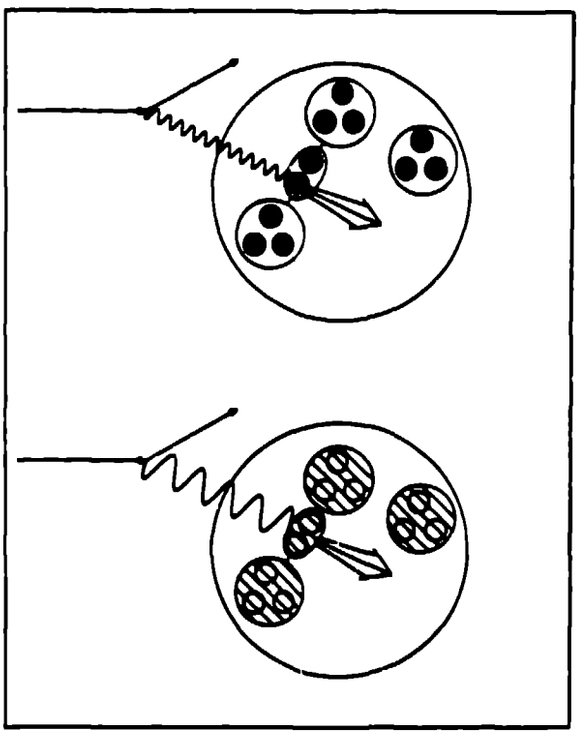

Fig. 11. Schematic representation of high-energy scattering probing the distributions of quarks and antiquarks (top) and medium-energy scattering probing the distributions of mesons and nucleons (bottom).

REFERENCES

1. J. B. McClelland et al., Phys. Rev. Lett. 53:144 (1984).
2. T. A. Carey et al., Phys. Rev. Lett. 49:266 (1982).
3. T. N. Taddeucci et al., Phys. Rev. Lett. 52:1960 (1984).
4. T. A. Carey, J. B. McClelland, E. J. Stephenson, and T. N. Taddeucci, IUCF Proposal 233 (unpublished).
5. J. M. Moss, "International Conference on Spin Excitations in Nuclei, eds. F. Petrovich et al., Plenum Press, New York, p. 355 (1984); J. M. Moss, Phys. Rev. C26:2063 (1982).
6. E. Bleszynski et al., Phys. Rev. C26:2063 (1982).
7. J. R. Shepard, International Conference on Antinucleon and Nucleon-Nucleus Interactions, Telluride, Colorado, March 1985, proceedings to be published.
8. J. A. McNeil, Proceedings of the LAMPF Workshop on Dirac Approaches to Nuclear Physics, Los Alamos, New Mexico (January 1985), Los Alamos Report LA-10438-C, p. 160.
9. S. J. Seestrom-Morris et al., Phys. Rev. C26:2131 (1982).
10. S. K. Nanda et al., Phys. Rev. Lett. 51:1526 (1983).
11. T. A. Carey, Invited talk at the 6th International Symposium on Polarization Phenomena in Nuclear Physics, Osaka, Japan (August 1985), proceedings to be published.
12. T. N. Taddeucci, ibid, Ref. 11.
13. S. J. Wallace, ibid, Ref. 8.
14. W. G. Love and Amir Klein, ibid, Ref. 8.

W. G. Love and J. R. Comfort, Phys. Rev. C29:2135 (1984).
15. D. A. Sparrow et al., Phys. Rev. Lett. 54:2207 (1985).
16. J. J. Aubert, et al., Phys. Lett. 123B:275 (1983).
17. C. H. Llewellyn-Smith, Phys. Lett. 128B:107 (1983).
18. M. Ericson and A. W. Thomas, Phys. Lett. 128B:112 (1983).
M. Ericson, Lecture Notes, International School of Physics, Erice, Italy, CERN preprint TH-3625.
A. W. Thomas, Univ. of Alberta/TRIUMF Workshop on Studying Nuclei with Medium Energy Protons, Edmonton, Alberta 1983, TRIUMF Report No. TRI-83-3.
19. D. Stump, G. F. Bertsch, and J. Pumplin, preprint.
20. E. L. Berger, F. Coester, and R. B. Wiringa, Phys. Rev. D29:398 (1984).
21. $x = Q^2/2m_N\omega$ where Q is the four-momentum transfer, m_N the nucleon mass, and ω the lepton energy loss.
22. F. E. Close, "An Introduction to Quarks and Partons," Academic Press, London, New York, and San Francisco.
23. T. A. Carey et al., Phys. Rev. Lett. 53:144 (1984).
24. G. F. Bertsch and O. Scholten, Phys. Rev. C25:804 (1982).
25. H. Esbensen and G. F. Bertsch, Ann. Phys. 157:255 (1984).
26. J. M. Moss et al., Phys. Rev. Lett. 48:789 (1982).
27. Z. E. Meziani et al., Phys. Rev. Lett. 54:1233 (1985).
28. W. M. Alberico, M. Ericson, and A. Molinari, Nucl. Phys. A379:429 (1982).
29. W. M. Alberico, M. Ericson, and A. Molinari, Phys. Rev. C30:1776 (1984).
30. J. Speth et al., Nucl. Phys. A343:383 (1980);
M. Rho, to be published in Ann. Rev. Nucl. Sci.;
G. E. Brown, private communication.
31. Calculations performed with the Los Alamos version of ISABEL by Y. Yariv and Z. Fraenkel;
Y. Yariv and Z. Fraenkel, Phys. Rev. C24:488 (1981).
32. L. B. Rees et al., to be published.
33. R. A. Arndt and D. Roper, Virginia Polytechnic Institute Scattering Analysis Interactive Dial-In Program, solution SP84.
34. H. Toki, G. F. Bertsch, and D. Cha, Phys. Rev. C28:1398 (1983).
35. C. H. Llewellyn-Smith, Nucl. Phys. A434:35c (1984).
36. H. Esbensen and G. F. Bertsch, preprint.
37. A. W. Thomas, private communication.